



## WEDNESDAY SLIDE CONFERENCE 2022-2023

Conference #15

11 January 2023

### CASE I:

#### **Signalment:**

3-month-old, male, Lewis rat (*Rattus norvegicus*)

#### **History:**

This rat was part of a study receiving high-dose whole body irradiation daily for six days. Five days after the last exposure, the animal presented quiet, with thin body condition (BSC 1/5), a hunched appearance, and an unkempt haircoat. Due to lack of improvement with supportive care, the animal was euthanized two days later and submitted for necropsy evaluation.

#### **Gross Pathology:**

On gross examination, the cecum was slightly distended and doughy, and there was a small amount of fecal staining at the ventral tail base. There were several formed fecal pellets present in the colon. The liver was mildly and diffusely pale.

#### **Laboratory Results:**

On CBC analysis, there was mild lymphopenia, mild neutrophilia, and moderate monocytosis. In addition, there was a mild decrease in HCT and MCV, and a mild increase in MCHC, representing a microcytic, hypochromic anemia.

#### **Microscopic Description:**

In sections of small intestine, there was loss of normal villus architecture characterized by moderate and multifocal villus blunting and

fusion, with replacement of areas of lamina propria with loose collagen and granulation tissue. The deep crypt epithelium was hyperplastic with large, plump crypt epithelial cells that showed piling and disorganization with frequent mitotic figures. Within the ileum, similar changes were present within the lamina propria and crypt epithelium, with the additional finding of severe, locally extensive mucosal ulceration with replacement by granulation tissue. There was diffuse and moderate lymphangiectasia within small intestinal villi and marked depletion of mucosal associated lymphoid tissue. Within the colon, there was marked degeneration and necrosis of the superficial mucosal and deep glandular epithelium with the presence of necrotic debris present within glandular lumens. There was moderate granulation tissue throughout the lamina propria of the colon, with attenuation, loss, and regeneration of colonic glandular epithelium. There was mild edema present within the submucosa, and severe lymphoid depletion within Peyer's patches. In the cecum, there were sporadic areas of glandular degeneration with loss of epithelium and small amounts of granulation tissue within the lamina propria. In other organs, there was



**Figure 1-1. Colon, intestine, rat. Three sections of colon (from left) and one section of intestine are submitted for examination. Dilated colonic glands are visible at subgross magnification. (HE, 6X)**

minimal and multifocal myofiber degeneration representative of chronic cardiomyopathy in the heart, sporadic clusters of alveolar histiocytes within the lung, and decreased erythroid progenitors within the bone marrow.

**Contributor’s Morphologic Diagnoses:**

Small and large intestine: Enterocolitis, necrotizing and ulcerative, diffuse, with regeneration.

**Contributor’s Comment:**

This case represents lesions which result from radiation toxicity to the intestinal tract. The lesions observed here are a continuum of glandular epithelial necrosis, regeneration, and ultimately, villar blunting, fusion, and granulation tissue proliferation as a result of cytotoxicity of rapidly dividing crypt epithelial cells. In humans, radiation-induced gastrointestinal syndrome (RIGS) occurs secondary to radiation therapy for neoplasia of the abdomen and pelvis and is a major limiting factor and source of morbidity and mortality in patients receiving this therapy.

The detrimental effects of radiation exposure were first described by Walsh (1897) two years after the discovery of X-rays, who concluded that irradiation caused inflammation of the mucosa of the intestinal tract.<sup>2,16</sup> Mechanisms underlying this side effect of radiation are still incompletely understood, and there are still no effective preventions or

treatments for this condition. Every year, over 300,000 patients receive abdominal radiation for cancer treatment, and approximately 60-80% of these patients develop some form of bowel toxicity.<sup>2,8</sup> In the process of radiation treatment for intra-abdominal or pelvic neoplasia, healthy bowel is ultimately affected by the radiation treatment, resulting in significant morbidity and mortality.<sup>13</sup> Therefore, it is a significant limiting factor for many patients receiving radiation therapy for abdominal or pelvic neoplasia.<sup>19,26</sup> However, radiation therapy is still a mainstay of cancer treatment, used in approximately half of cancer patients, and is therapeutically critical in ~25% of cancer cures so a better understanding of mechanisms behind RIGS and preventative measures against it are critical.<sup>8</sup>

In acute cases of RIGS, the intestine represents an important organ at early risk, because of the nature of intestinal biology. While the pathophysiology of RIGS is still not fully understood, data suggests that it arises from a complex interaction of epithelial damage, and alterations in the immune, vascular, and enteric nervous systems, influenced by host (co-morbidities such as IBD, diabetes, vascular or collagen disorders, genetic predisposition, body mass index, tobacco smoking, genetic disorders) and therapeutic factors (dose of radiation, length of bowel involved, concurrent chemotherapy, abdominal surgery).<sup>8,13</sup> Intestinal epithelium, particularly intestinal stem cells (ISCs) have a high rate of proliferation and thus make the bowel a sensitive target for radiation toxicity.<sup>13</sup> In acute RIGS, this phase occurs immediately following exposure and may persist for hours to several days, and results from a direct cytotoxic effect of radiation resulting in cytotoxicity of crypt epithelial cells, including stem cells, which results in epithelial cell loss, villus blunting, fusion, and impairment of epithelial barrier function with loss of electrolytes, water, protein, mucosal

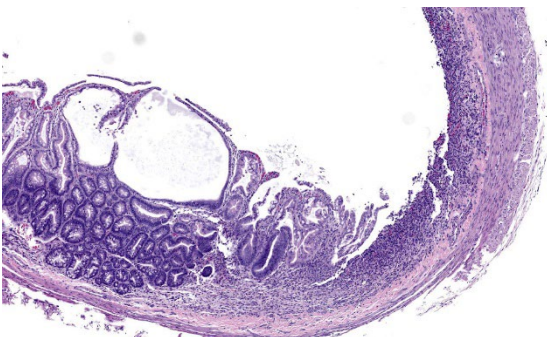


**Figure 1-2. Colon, rat. There is a segmental area of ulceration (right), with ectatic glands at the periphery. (HE, 52X)**

ulceration, and increased permeability to luminal pathogens and antigens, resulting in mucosal inflammation and ultimately systemic effects of sepsis.<sup>2,8,13,16</sup> Compromise to the vascular architecture leads to hemorrhage and thrombosis, which precedes ischemic damage; in addition, several animal studies have shown a direct effect on the enteric nervous system, resulting in reduced transit time and intestinal ileus.<sup>13</sup>

As lesions progress, acute RIGS may resolve following cessation of radiation exposure, or in some cases (often months to several years following exposure) may become a chronic condition, secondary to progressive occlusive vasculitis, extracellular matrix remodeling, and collagen deposition resulting in atrophy of the intestinal mucosa, fibrosis, structure formation, fistula development, and intestinal obstruction or perforation; the chronic form of RIGS occurs in up to ~17% of individuals treated with abdominal/pelvic irradiation.<sup>8,13,16</sup> In fact, a latency period of several decades (20-30 years) between radiation therapy and chronic RIGS is not an uncommon clinical phenomenon.<sup>8</sup>

While the pathophysiology of RIGS is poorly understood, a number of studies have shown a relationship between growth factor pathways, cell cycle proteins, DNA damage mediators, and developmental or stem cell pathways in the progression of disease. For example, radiation induced damage to the intestinal tract is associated with upregulation of the JNK-MAPK cell growth and proliferation pathways and decreased expression of stress-activated p38 MAPK pathways which are important for regeneration and repair of intestinal mucosal defects.<sup>26</sup> Inhibition of the cell cycle, either through cyclin/cdk complex inhibition, or modulation of cell cycle regulators and DNA damage checkpoint mediators, appears to protect against or improve response to GI toxicity; CDK4/6 inhibitors

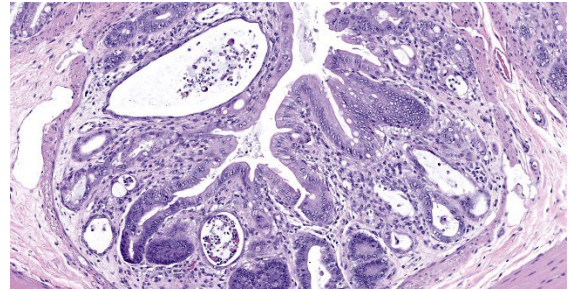


**Figure 1-3. Colon, rat. Dilated colonic glands are lined by attenuated epithelium and contain low numbers of necrotic epithelium and cellular debris. (HE, 158X)**

improve survival in irradiated mice by blocking crypt epithelial apoptosis and promoting epithelial cell survival and self-renewal through upregulation of stem cell factors (LGF5, BMI-1, Hopx, mTERT, Lrig1) and inhibiting radiation induced P53 apoptotic response.<sup>16,17,18,19,24</sup> Prophylactic therapy with various growth factors and cytokines such as TGF $\beta$ , IL-11, keratinocyte growth factor (KGF), and Kruppel-like factor (KLF) increases crypt survival following radiation.<sup>1,2,7,15</sup> Radiation induced injury to the intestinal tract is also associated with increased levels of oxidative tissue injury, and studies have shown that certain antioxidants and mediators of oxidative stress play a role in RIGS and its progression. For example, cyclooxygenase induced prostaglandins prevent cytotoxicity of crypt epithelial cells in mice,<sup>16</sup> and alterations in the mTOR-PI3K and NRF2 pathways regulating oxidative stress can protect the intestinal tract through mediation of oxidative stress and upregulation of stem cell factors and growth pathways such as the NF- $\kappa$ B pathway.<sup>5,25</sup> Finally, blockage of the TLR pathway, important in promotion of inflammatory responses to microbial pathogens, protects from lethal radiation induced intestinal injury in mice.<sup>22</sup>

Since intestinal stem cells are a target of radiation induced toxicity, activation of developmental and stem-cell embryonic pathways have shown to be effective in mediating RIGS in animal models, as epithelial regeneration following radiation injury requires

intestinal stem cell repopulation.<sup>12,14,19</sup> For example, activation of the Wnt/beta-catenin pathway or suppression of the adenomatous polyposis coli (Apc) gene function in radiation injury stimulates repair and significantly improves morbidity and mortality in mice following high dose radiation.<sup>19</sup> Notch signaling, another developmental/stem cell pathway, regulates self-renewal of intestinal stem cells and activation of this pathway accelerates reversal of radiation induced damage in the intestinal tract.<sup>14</sup> Mesenchymal stem cells, or stromal progenitor cells (SPCs) have been shown to have regenerative, immune modulatory, angiogenic, and anti-inflammatory properties that promote healing.<sup>3,21</sup> In addition, the recruitment of extra-intestinal and bone marrow-derived cells has been shown to play a role in promotion of intestinal healing and improvement of morbidity and mortality in radiation-induced intestinal injury through secretion of growth factors, stem cell mediators, and inflammatory cytokines in a paracrine fashion.<sup>21</sup>

Lastly, there is a significant role of the microbiome in the response to RIGS.<sup>8,13</sup> Radiation of the intestinal tract results in alterations in normal intestinal microbiota, which is an important factor in the pathogenesis of radiation enteritis; radiation reduces the normal diversity of the gut microbiota and leads to dysbiosis, which aggravates RIGS by weakening intestinal epithelial barrier function and promoting inflammation.<sup>4,9</sup> Changes in the microbiome of the intestine reflect altered

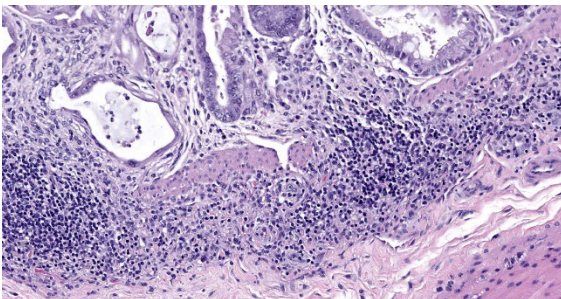


**Figure 1-4.** Colon, rat. Beneath affected glands, lymphocyte numbers in Peyer's patches are markedly diminished. (HE, 241X)

diversity reflective of decreased beneficial *Lactobacillus* and *Bacterioides* spp. and increased *E. coli* and *Streptococcus* spp.<sup>23,26</sup> As a further result of altered diversity of microbes, the composition of short-chain fatty acids (SCFAs), the key metabolites generated by large intestinal microbial metabolism, is altered as well; SCFAs play an important role in intestinal repair, inflammation, and homeostasis in the gut.<sup>26</sup> Transplantation of normal fecal microbiota has been shown to improve survival in irradiated animals and improve overall function of the intestinal tract.<sup>4</sup> Dysbiosis also promotes inflammation and alterations in barrier function in the intestinal tract, influenced by enhanced pro-inflammatory cytokine signaling through TNF $\alpha$  and IL1 $\beta$  expression, and rearrangement of important tight junction proteins induced by microbes such as pathogenic *E. coli*.<sup>9,23</sup> In fact, beneficial effects on intestinal symptoms have been observed using probiotics including *Lactobacillus* in animal models and humans in reducing endotoxin levels, reduction in severity of bowel injury, and reduction in potential bacteremia.<sup>13</sup>

In summary, a full understanding of the pathophysiology of radiation induced injury in the intestinal tract is still incomplete, but likely involves a complex interplay between epithelial damage and repair, induction of developmental and stem cell pathways, growth factors and cell cycle/DNA damage mediators, the inflammasome, endothelial injury, tissue remodeling, and effects on the enteric nervous system, influenced by alterations in normal gut microbiota to result in the clinical syndrome of RIGS.

#### **Contributing Institution:**

In Vivo Animal Core, Unit for Laboratory Animal Medicine  
University of Michigan Medicine  
North Campus Research Complex, Building 36, Rm G177

2800 Plymouth Road  
Ann Arbor, MI 48109

**JPC Diagnosis:**

1. Colon: Colitis, necrotizing, multifocal to coalescing with glandular regeneration and lymphoid depletion.
2. Small intestine: Enteritis, necrotizing, segmental, moderate, with ulceration, crypt abscesses, and crypt hyperplasia.

**JPC Comment:**

The contributor provides an excellent description of radiation-induced gastrointestinal syndrome. To see the effects of ionizing radiation on the lung, WSC 2021, Conference 17, Case 4 is a case of radiation pneumonitis in a rhesus macaque exposed to whole thorax radiation, and the contributor described the pathogenesis behind acute and chronic phases of injury.

This week's moderator, Dr. Cory Brayton of Johns Hopkins University School of Medicine, commented on the atypical features of regeneration in this case, including anisocytosis, anisokaryosis, and presence of goblet cells in the crypts, which provide clues as to

pathogenesis of this case. IBA-1 revealed the scattered inflammatory infiltrate in the lamina propria to be composed of abundant macrophages called into clean up necrotic cellular debris.

Additionally, she pointed out a histoanatomic feature which is helpful identifying origin of a colonic section: the mucosal folds in present in the colonic section in this case are more prominent in the proximal section of the colon and correspond to grossly visible diagonal lines on the serosal surface.

Acute radiation syndrome occurs after exposure to a substantial amount of ionizing radiation and may occur as a result of radiotherapy/radiopharmaceuticals, nuclear accidents, or atomic bombings. The effects are dependent on both the dose and type of radiation and regions and proportion of the body exposed. Systems particularly sensitive to acute radiation injury include the hematopoietic, gastrointestinal, integumentary, and nervous systems. The prodrome phase of ARS occurs immediately after exposure and results in nausea, vomiting, fatigue, or loss of consciousness from autonomic stability.<sup>6</sup> This is

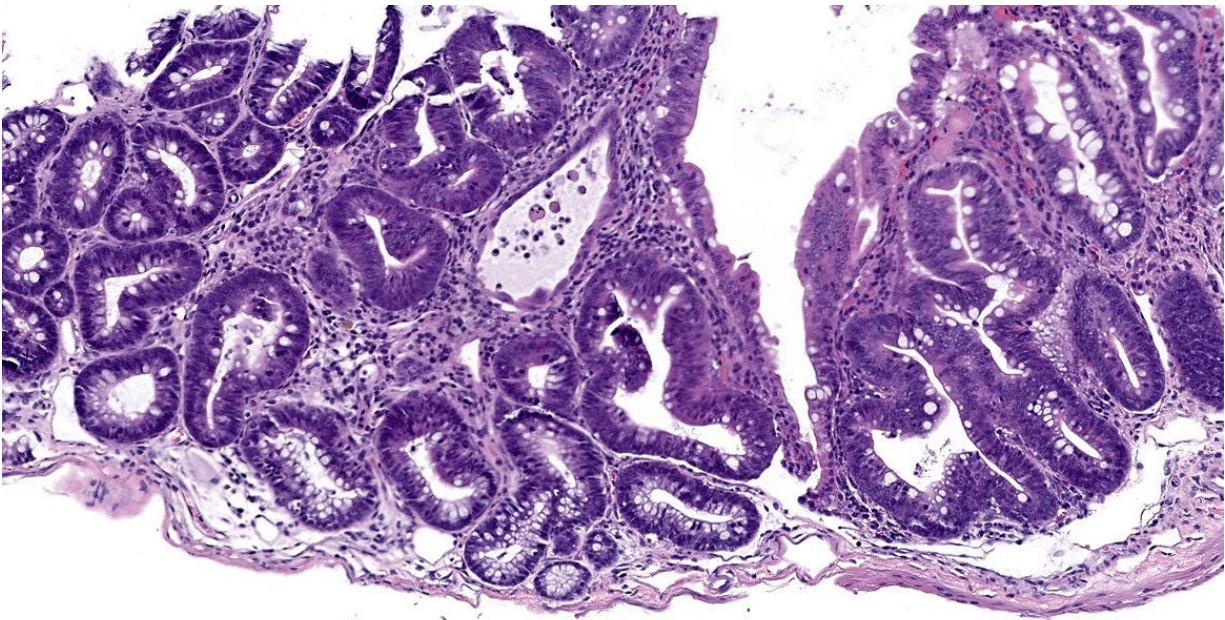
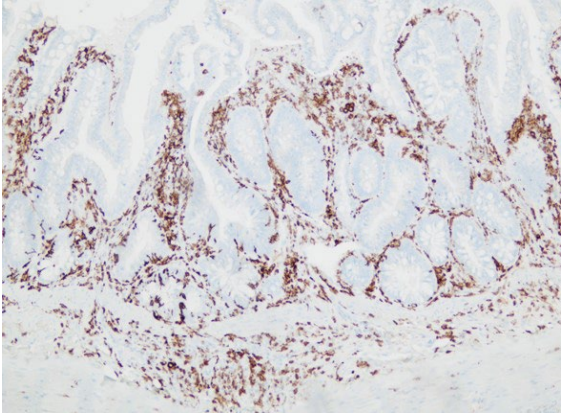


Figure 1-5. Intestine, rat. There are necrotic crypts within the intestinal mucosa as well. (HE, 241X)



**Figure 1-6.** *There are numerous macrophages infiltrating the lamina propria of irradiated segments of intestine. (IBA-1, 200X)*

followed by a variable and dose-dependent latent period followed by manifest illness.<sup>6</sup> Apoptosis of myeloid precursors in bone marrow and peripheral leukocytes (particularly lymphocytes) leads to cytopenias.<sup>6,11</sup> Thrombocytopenia results in hemorrhage, while lymphopenia and neutropenia impair immune function.<sup>6,11</sup> Radiation induced gastrointestinal system leads to transmigration of bacteria and subsequent septicemia.<sup>6</sup> At higher levels of exposure, neurologic injury and hemorrhage injury occurs.<sup>6,11</sup>

The radiation exposure level required to induce clinical signs is variable between species and between individuals. The LD50/30, or the dose where 50% of animals survive 30 days without medical care, varies from as little as 2.5 Gy in swine to up to 10 Gy in Mongolian gerbils.<sup>6</sup> For reference, 1 Gy is approximately 300 times the annual background radiation exposure of a person in the US.<sup>20</sup>

Severity of radiation injury is compounded when it is followed by or simultaneous with other trauma (i.e. thermal burns, wounds).<sup>6,11</sup> In a canine study, thermal burns covering 20% of the body resulted in minimal mortality, but when combined with 1 Gy exposure, burns of the same extent caused 73% mortality.<sup>6</sup> This compounded effect is attributed, at least in part, to delayed wound healing and acute immunosuppression from radiation

injury.<sup>6,11</sup> The likelihood of polytrauma in radiation exposure secondary to nuclear weapon detonation is high: approximately 70% of atomic bomb survivors in Hiroshima and Nagasaki and 10% of Chernobyl nuclear accident survivors experienced combined injuries.<sup>11</sup>

Effects of acute radiation syndrome are considered deterministic, as exposure above a certain threshold produces these injuries consistently as a result of direct cellular damage and tissue reactions.<sup>10</sup> Deterministic effects may occur acutely or have a late onset.<sup>10</sup> Stochastic effects, on the other hand, tend to have a late onset and are the result of genetic damage. These do not occur as consistently as deterministic effects; rather, the incidence of disease increases proportionally with the degree of exposure. An example of a stochastic effect is an increased risk of cancer due to mutations in somatic cell DNA; hereditary effects also occur as a result of mutations in germline cells.<sup>10</sup>

Long term stochastic effects of radiation exposure have been extensively documented in the Life Span Study, a decades-long and ongoing study evaluating the medical outcomes of 93,741 atomic bombing survivors from Hiroshima and Nagasaki and 26,580 unexposed cohorts.<sup>20</sup> The earliest stochastic effect was an increase in rates of leukemia seen within two years of the bombings. Since then, the study has uncovered a significant linear and dose dependent increase in the occurrence of cancers in multiple locations, including the stomach, lung, liver, colon, thyroid, and skin.<sup>20</sup> Risks of death due to solid cancers, stroke, and heart disease are significantly increased in exposed individuals.<sup>20</sup> The study also found a decrease rate of growth in those who were 5-15 years old at the time of the bombings.<sup>20</sup>

## References:

1. Boerma M, Wang J, Sridharan V, Herbert JM, Hauer-Jensen M. Pharmacological induction of transforming growth factor-beta1 in rat models enhances radiation injury in the intestine and the heart. *PLoS One*. 2013;8: e70479.
2. Booth C, Tudor G, Tudor J, Katz BP, MacVittie TJ. Acute gastrointestinal syndrome in high-dose irradiated mice. *Health Phys*. 2012;103: 383-399.
3. Chang PY, Zhang BY, Cui S, et al. MSC-derived cytokines repair radiation-induced intra-villi microvascular injury. *Oncotarget*. 2017;8: 87821-87836.
4. Cui M, Xiao H, Li Y, et al. Faecal microbiota transplantation protects against radiation-induced toxicity. *EMBO Mol Med*. 2017;9: 448-461.
5. Datta K, Suman S, Fornace AJ, Jr. Radiation persistently promoted oxidative stress, activated mTOR via PI3K/Akt, and downregulated autophagy pathway in mouse intestine. *Int J Biochem Cell Biol*. 2014;57: 167-176.
6. DiCarlo AL, Maher C, Hick JL, et al. Radiation Injury After A Nuclear Detonation: Medical Consequences and the Need for Scare Resources Allocation. *Disaster Med Public Health Prep*. 2011; 5 Suppl 1: S32-44.
7. Farrell CL, Bready JV, Rex KL, et al. Keratinocyte growth factor protects mice from chemotherapy and radiation-induced gastrointestinal injury and mortality. *Cancer Res*. 1998;58: 933-939.
8. Hauer-Jensen M, Denham JW, Andreyev HJ. Radiation enteropathy--pathogenesis, treatment and prevention. *Nat Rev Gastroenterol Hepatol*. 2014;11: 470-479.
9. Jian Y, Zhang D, Liu M, Wang Y, Xu ZX. The Impact of Gut Microbiota on Radiation-Induced Enteritis. *Front Cell Infect Microbiol*. 2021;11: 586392.
10. Kamiya K, Ozasa K, Akiba S, et al. Long-term effects of radiation exposure on health. *Lancet*. 2015; 386: 469-478.
11. Kiang JG, Olabisi AO. Radiation: a poly-traumatic hit leading to multi-organ injury. *Cell Biosci*. 2019; 9(25):1-15.
12. Kulkarni S, Wang TC, Guha C. Stromal Progenitor Cells in Mitigation of Non-Hematopoietic Radiation Injuries. *Curr Pathobiol Rep*. 2016;4: 221-230.
13. Kumagai T, Rahman F, Smith AM. The Microbiome and Radiation Induced-Bowel Injury: Evidence for Potential Mechanistic Role in Disease Pathogenesis. *Nutrients*. 2018;10.
14. Kwak SY, Shim S, Park S, et al. Ghrelin reverts intestinal stem cell loss associated with radiation-induced enteropathy by activating Notch signaling. *Phytomedicine*. 2021;81: 153424.
15. Li M, Gu Y, Ma YC, et al. Kruppel-Like Factor 5 Promotes Epithelial Proliferation and DNA Damage Repair in the Intestine of Irradiated Mice. *Int J Biol Sci*. 2015;11: 1458-1468.
16. MacNaughton WK. Review article: new insights into the pathogenesis of radiation-induced intestinal dysfunction. *Aliment Pharmacol Ther*. 2000;14: 523-528.
17. Metcalfe C, Kljavin NM, Ybarra R, de Sauvage FJ. Lgr5+ stem cells are indispensable for radiation-induced intestinal regeneration. *Cell Stem Cell*. 2014;14: 149-159.
18. Pant V, Xiong S, Wasylshen AR, et al. Transient enhancement of p53 activity protects from radiation-induced gastrointestinal toxicity. *Proc Natl Acad Sci U S A*. 2019;116: 17429-17437.
19. Romesser PB, Kim AS, Jeong J, Mayle A, Dow LE, Lowe SW. Preclinical murine platform to evaluate therapeutic countermeasures against radiation-induced gastrointestinal syndrome. *Proc Natl Acad Sci U S A*. 2019;116: 20672-20678.
20. Sakata R, Grant EJ, Ozasa K. Long-term follow-up of atomic bomb survivors. *Maturitas*. 2012; 72: 99-103.

21. Sung J, Sodhi CP, Voltaggio L, et al. The recruitment of extra-intestinal cells to the injured mucosa promotes healing in radiation enteritis and chemical colitis in a mouse parabiosis model. *Mucosal Immunol.* 2019;12: 503-517.
22. Takemura N, Kawasaki T, Kunisawa J, et al. Blockade of TLR3 protects mice from lethal radiation-induced gastrointestinal syndrome. *Nat Commun.* 2014;5: 3492.
23. Wang Z, Wang Q, Wang X, et al. Gut microbial dysbiosis is associated with development and progression of radiation enteritis during pelvic radiotherapy. *J Cell Mol Med.* 2019;23: 3747-3756.
24. Wei L, Leibowitz BJ, Wang X, et al. Inhibition of CDK4/6 protects against radiation-induced intestinal injury in mice. *J Clin Invest.* 2016;126: 4076-4087.
25. Yang W, Sun Z, Yang B, Wang Q. Nrf2-Knockout Protects from Intestinal Injuries in C57BL/6J Mice Following Abdominal Irradiation with gamma Rays. *Int J Mol Sci.* 2017;18.
26. Zhu S, Liang J, Zhu F, et al. The effects of myeloablative or non-myeloablative total body irradiations on intestinal tract in mice. *Biosci Rep.* 2021;41.

## **CASE II:**

### **Signalment:**



**Figure 2-1. Liver, mouse. Three sections of the liver are submitted for examination. There are no changes evident at subgross magnification. (HE, 6X)**

Three ~12-week-old male mice (*Mus musculus*) on a C57BL/6J background were evaluated.

### **History:**

Mice were heterozygous knockouts for a gene involved in tRNA modification\* and had no clinically detectable phenotype. The mutation had been generated in C57BL/6J mice (B6J) and backcrossed to wild-type B6J.

*\*The phenotype of this mutation is as yet unpublished, and permission has not been granted to reveal the specific gene.*

### **Gross Pathology:**

Two of the three male mice had small livers at necropsy.

### **Laboratory Results:**

No laboratory findings reported.

### **Microscopic Description:**

In the livers of all three mice, portal veins were diffusely absent or small and slit-like. Portal triads frequently contained multiple hepatic arteriolar profiles (arteriolar reduplication), many of which had thickening of the tunica media. Periportal lymphatics were dilated and prominent and mild dilation of hepatic sinusoids was also present multifocally. Two of the three mice also had multifocal, random and perivascular small aggregates of infiltrating leukocytes, sometimes accompanied by focal loss or degeneration of hepatocytes. Infiltrating leukocytes consisted of mononuclear cells and, less frequently, neutrophils.

### **Contributor's Morphologic Diagnoses:**

Liver:

1. Portal vein hypoplasia, diffuse, severe, with lymphatic ectasia and arteriolar reduplication
2. Mononuclear and neutrophilic infiltration, random and perivascular, mild

### Contributor's Comment:

Portal vein hypoplasia is the histologic manifestation of intra or extrahepatic portosystemic shunting (PSS).<sup>1,4</sup> In dogs, the term microvascular dysplasia (MVD) has been used to describe histologic findings of PSS in the absence of a detectable shunt but, because the histology and pathogenesis of MVD overlap with that of congenital PSS, the morphologic diagnosis of portal hypoplasia is now preferred for both conditions according to the World Small Animal Veterinary Association.<sup>4</sup> Portal vein hypoplasia is characterized by absent or slit-like portal vein profiles and increased hepatic arteriolar profiles, or arteriolar reduplication. Arteriolar reduplication can occur with portal hypertension<sup>6</sup>, however congenital PSS lacks portal hypertension and, as in this submission, associated changes of portal fibrosis may be absent. In PSS, arteriolar duplication may represent a compensatory response to decreased portal delivery of trophic factors to hepatocytes.<sup>1</sup>

Spontaneous congenital portosystemic shunting (PSS) with a microscopic appearance similar to this submission was recently described in a fairly high (~25%) number of C57BL6/J mice.<sup>2</sup> Affected mice were both transgenic and wild-type and originated from multiple different institutions, thus the finding was believed to be background strain-related. Shunting was not visible grossly and was confirmed by microscopy and by specialized imaging of blood flow through the liver. Based on shunt location (within the left side of the liver), pathogenesis was speculated to involve persistence of the ductus venosus (shunts blood from placenta to vena cava in the fetus). Inheritance was non-Mendelian and epigenetic alterations were suspected. As is typical of PSS in dogs, bilirubin, alanine aminotransferase (ALT), and aspartate aminotransferase (AST) remained within historic reference intervals, although affected

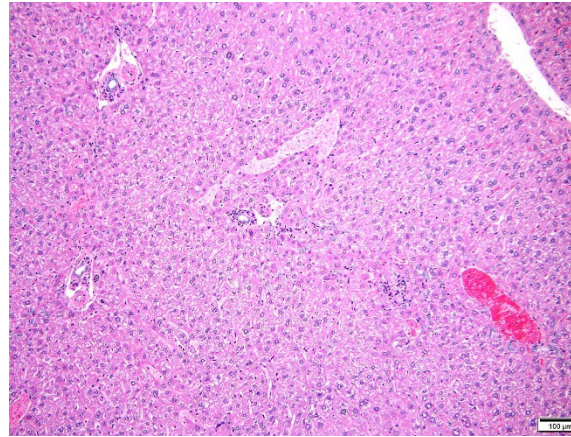


**Figure 2-2. Liver, mouse. Hepatic lobules are decreased in size; portal triads are in close proximity. (HE, 100X)** (Photo courtesy of: University of Michigan Unit for Laboratory Animal Medicine In Vivo Animal Core (IVAC) <https://animalcare.umich.edu/business-services/vivo-animal-core>)

mice had greater variation in AST and ALT. Bile acids may be more diagnostic but are not routinely performed in mice. Of note, affected mice were originally identified by an abnormal brain neurochemical profile (elevated glutamine) during screening by proton magnetic resonance spectroscopy. Glutamine is an end-product of ammonia detoxification by astrocytes in hepatic encephalopathy. Although symptoms of hepatic encephalopathy were not described, elevation of brain glutamine levels correlated with portosystemic shunting and may indicate some level of subclinical metabolic encephalopathy.<sup>2</sup> Thus, altered metabolism and/or neurochemistry in B6J mice with this defect may affect their suitability for research.

Based on this previous report, intrahepatic shunting may be more common than typically realized in mice and caution is warranted in specifically ascribing a finding of portal hypoplasia to genetic manipulation. In this submission, it was not possible to determine whether portal vein hypoplasia was related to the knockout gene, but spontaneous occurrence was suspected due to the background strain and the lack of a biologically plausible link between the knockout to the lesion. It is intriguing that the lesion was

present in 3 of 3 male but 0 of 3 female heterozygotes, however the knockout was not restricted to the liver nor was a sex-linked or liver-restricted phenotype expected. Other mice from the strain were not available for evaluation. No clinical signs suggestive of symptomatic portosystemic shunting (neurological symptoms, small size) were seen, although 2 of the male mice were noted to have small livers at necropsy.

Small foci of random or perivascular infiltrating leukocytes as seen in these mice are common murine background findings. Since they were occasionally accompanied by hepatocyte loss, they may have been exacerbated in this case by decreased trophic supply of nutrients to hepatocytes due to portal hypoplasia.

**Contributing Institution:**

University of Michigan Unit for Laboratory Animal Medicine In Vivo Animal Core (IVAC) <https://animalcare.umich.edu/business-services/vivo-animal-core>

**JPC Diagnosis:**

Liver, portal areas: Venous hypoplasia, multifocal.

**JPC Comment:**

The histologic appearance in this case is characteristic of portal vein hypoperfusion: decreased portal vein profiles, increased numbers of arteriolar profiles due compensatory hyperperfusion, and hepatocellular atrophy with irregularly spaced small portal triads. Portal vein hypoperfusion can also feature periportal fibrosis, biliary ductular reaction, and lipogranulomas.<sup>3,4</sup>

Portal vein hypoperfusion is the non-specific result of several distinct diseases. In many of these conditions, hypoperfusion is the result of portal hypertension, which can result in ascites, a useful distinguishing clinical characteristic. Examples of diseases which produce portal hypertension include arterioportal fistulas, obstruction of the portal vein, and primary portal vein hypoplasia.<sup>4</sup> Obstruction of the portal vein may occur due to thrombosis or neoplasia and leads to decreased portal blood flow and hypoperfusion. In arteriovenous fistulas, blood travels from a higher-

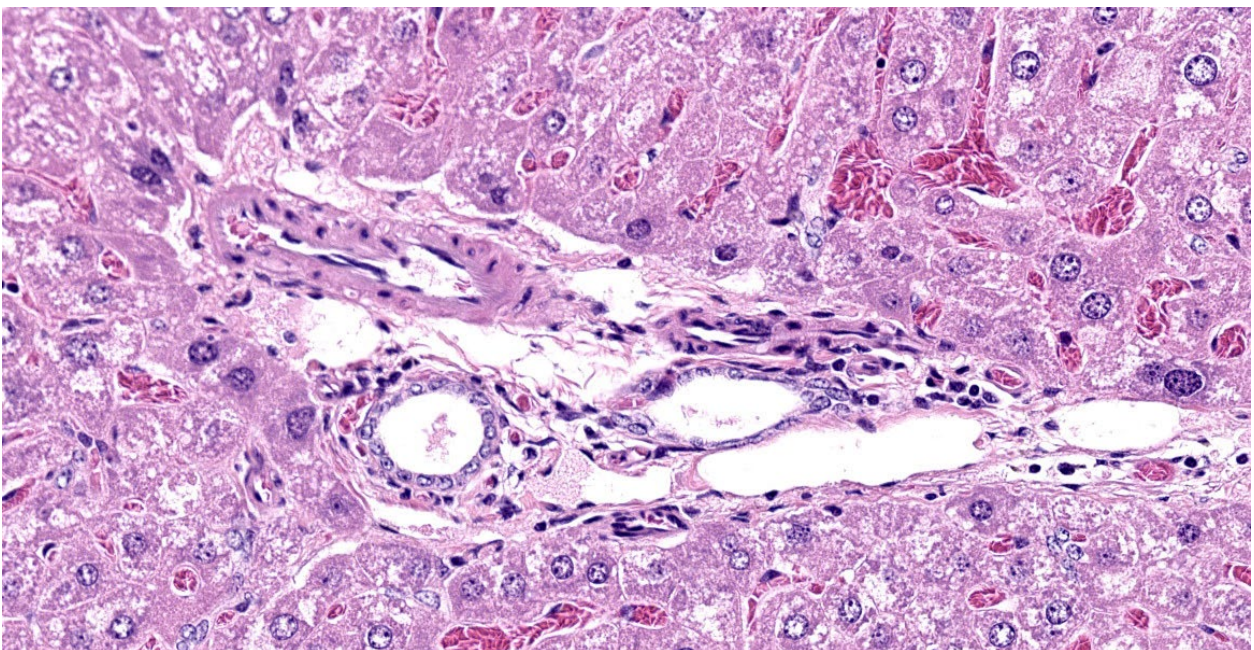


*Figure 2-3. Liver, mouse. Portal areas contain multiple sections of arterioles, bile ducts, and dilated lymphatics. Portal venules are not evident. (HE, 381X)*

pressure artery into the portal vein, leading to retrograde venous blood flow. While the directly affected lobe contains venous aneurysmal dilations and thick tortuous arteries, subsequent portal hypertension causes characteristic portal vein hypoperfusion in the unaffected lobes. Primary hypoplasia of the portal vein may occur in extrahepatic or intrahepatic locations. Some forms are mild, and histologic lesions are limited to those of hypoperfusion; moderate to severe forms are characterized by portal fibrosis and portal hypertension.

The end result of portal hypertension is acquired portosystemic shunting of blood, where blood flows through numerous enlarged and tortuous collateral veins to reach systemic circulation. Congenital portosystemic shunts, on the other hand, characteristically lack portal hypertension. The flow of blood bypasses the liver, traveling directly from portal vessels to the caudal vena cava or azygous vein and causing portal vein hypoperfusion.

Several features of portosystemic shunts in C57BL/6J mice were described in a recent study evaluating the effect of portal circulation in non-alcoholic fatty liver disease.<sup>5</sup> In PSS mice, the hepatic surface was faintly nodular and dull compared to normal livers.<sup>5</sup> Staining with pimonidazole, a hypoxia marker, revealed strong staining in the centrilobular region but negative staining in the portal regions, illustrating that arteriolar compensation for portal hypoperfusion was not able to fully oxygenate the distant centrilobular zone.<sup>5</sup> When given the hepatotoxin carbon tetrachloride, PSS mice had less hepatic injury than non-PSS mice.<sup>5</sup> This was previously reported to be due to decreased CYP2E1 expression; however, this study found CYP2E1 expression was increased in PSS mice and the authors speculated that

decreased oxygen availability from hypoxia may have reduced free radical generation.<sup>5</sup>

The moderator described some of the porto-systemic shunts may have on research studies, including smaller livers, altered neurochemical phenotypes, and altered metabolism of drugs and xenobiotics. Participants also discussed the hepatocellular anisokaryosis, particularly in the mid-zonal regions, which is an incidental aging change due to polyploidy.

### **References:**

1. Baade S, Aupperle H, Grevel V, Schoon HA. Histopathological and immunohistochemical investigation of hepatic lesions associated with portosystemic shunting in dogs. *J Comp Pathol.* 2006;134:80-90.
2. Cudalbu C, McLin VA, Lei H, et al. The C57BL/6J mouse exhibits sporadic congenital portosystemic shunts. *PLoS One.* 2013; 8(7): e69782.
3. Cullen JM, Stalker MJ. Liver and biliary system. In: Maxie MG, ed. *Jubb, Kennedy and Palmer's Pathology of Domestic Animals.* Vol 2. 6th ed. St. Louis, MO: Elsevier Ltd; 2016:266-267,289-292
4. Cullen JM, van den Ingh TSGAM, Bunch SE, Rothuizen J, Washabau RJ, Desmet VJ: Morphological classification of the circulatory disorders of the canine and feline liver. In: *WSAVA Standards for Clinical and Histological Diagnosis of Canine and Feline Liver Diseases.* St. Louis, MO: Elsevier. 2006: 41-59, 97-98.
5. Meng L, Goto M, Tanaka H, et al. Decreased Portal Circulation Augments Fibrosis and Ductular Reaction in Nonalcoholic Fatty Liver Disease in Mice. *Am J Pathol.* 2021; 191(9):1580-1591.
6. Nakhleh RE. The pathological differential diagnosis of portal hypertension. *Clinical Liver Disease.* 2017;10(3):57-62.

### **CASE III:**

**Signalment:**

13-month-old, female-intact, Sprague-Dawley rat (*Rattus norvegicus*)

**History:**

Sentinel rat, presented with abdominal distention. On physical examination, the clinician palpated a freely moveable, large, firm mass within the peritoneal cavity.

**Gross Pathology:**

The animal is underconditioned (2/5 score). The right kidney is 2.834 g, the left kidney is 122.0 g. The mass is surrounded but not adhered to omentum. Approximately 90% of the right kidney is replaced by a 7 x 5.5 x 5 cm, discrete, encapsulated, semi-firm, pale-tan to brown to red, multilobular mass. On cut section, the mass is composed of smooth, homogeneous, pale-tan regions surrounding a friable, dark-red to brown core.

**Laboratory Results:**

Immunohistochemistry and special stains:

Vimentin: Strong, diffuse, cytoplasmic immunoreactivity of blastemal and stromal neoplastic populations. The primitive tubular epithelial structures are negative.

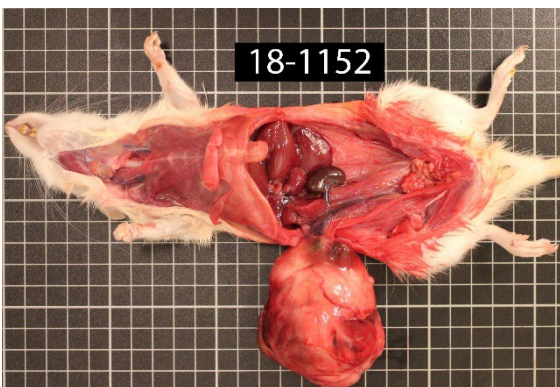


**Figure 3-1. Kidney, rat.** The right kidney is replaced by a multilobular, pale-tan to red to brown, irregular, smooth mass. Sprague-Dawley rat. (Photo courtesy of Laboratory of Comparative Pathology; Hospital for Special Surgery, Memorial Sloan Kettering Cancer Center, The Rockefeller University, Weill Cornell Medicine. <https://www.mskcc.org/research-areas/programs-centers/comparative-medicine-pathology>)

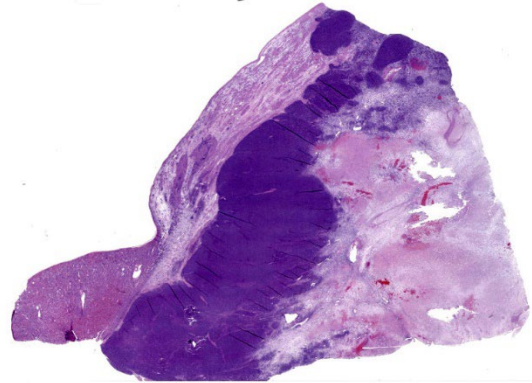


**Figure 3-2. Kidney, rat.** A section of kidney with a large unencapsulated mass is submitted for examination. (HE, 3X)

Cytokeratin wide-spectrum screening (WSS): Strong, diffuse, cytoplasmic immunoreactivity of tubular epithelial neoplastic cell populations. The blastemal and stromal components negative.

Wilms tumor protein (WT1): Moderate, diffuse, nuclear immunoreactivity of the blastemal with variable immunoreactivity of the stromal neoplastic population and rare, equivocal nuclear immunoreactivity of a few tubular structures.

N.b. Normal renal tubular and glomerular epithelium also has moderate, variable nuclear immunoreactivity.

Masson's Trichrome: Masson's trichrome confirms the presence of collagen within the tumor population (blue staining) and suggests differentiation into muscle (red staining).

**Microscopic Description:**

Arising from, compressing, and replacing approximately 50% of the renal parenchyma is a partially encapsulated, multilobular, ill-demarcated, expansile and densely cellular neoplasm that extends to cut borders. The neoplasm is composed of three haphazardly organized cell populations: epithelial, stromal and blastemal. The epithelial component is characterized by cuboidal to columnar cells which form tubules rimmed by a few layers of blastemal cells. The stromal population is

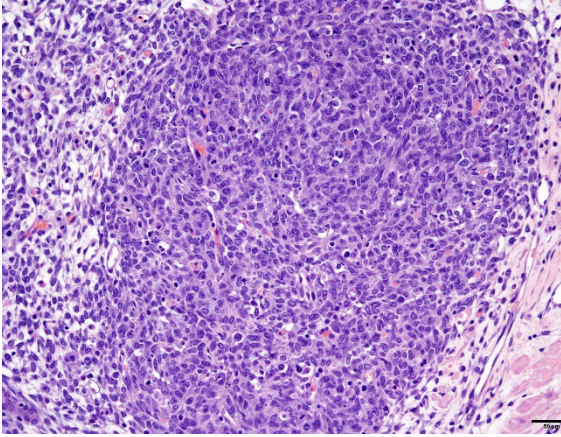


**Figure 3-3. Kidney, rat. The blastemal population is composed of dense streams of basophilic polygonal cells with scant cytoplasm, and indistinct cell borders. (HE, 400X) (Photo courtesy of Laboratory of Comparative Pathology; Hospital for Special Surgery, Memorial Sloan Kettering Cancer Center, The Rockefeller University, Weill Cornell Medicine. <https://www.mskcc.org/research-areas/programs-centers/comparative-medicine-pathology>)**

composed of fusiform cells arranged in bundles and are supported by a loose fibrovascular stroma. Multifocally, there is differentiation of the mesenchymal cells into collagen, striated and smooth muscle. The blastemal population is composed of dense streams of basophilic polygonal cells with scant cytoplasm, and indistinct cell borders. Anisocytosis and anisokaryosis are mild. The mitotic count in the blastemal population is high, but low in the other populations. The mass has large lakes of necrosis, hemorrhage, edema, fibrin and rare mineralization, admixed with large numbers of degenerate and non-degenerate neutrophils, macrophages, and lesser numbers of lymphocytes and plasma cells. Multifocally, vessels are partially occluded by fibrin thrombi. At the margins of the mass, scattered within the stromal population, are small numbers of misshapen, partially developed and variably sclerotic glomeruli, occasionally surrounded by an ectatic Bowman's space. Adjacent to these, there are small numbers of variably sized tubules, which are not surrounded by a rim of blastemal cells.

#### **Contributor's Morphologic Diagnoses:**

Kidney: Triphasic nephroblastoma with striated and smooth muscle differentiation (syn: Wilms Tumor)

#### **Contributor's Comment:**

A nephroblastoma, also known as a Wilms tumor (WT), is an undifferentiated, embryonal, mesodermal tumor with multipotent differentiation capabilities, that is thought to arise from the primitive renal stem cell.<sup>14</sup> It is the most common renal tumor in childhood.<sup>9</sup> In human pediatric patients, it is associated with germline and/or somatic mutations of the WT1 gene, but other genes are thought to be involved as well<sup>3</sup>. Precursor lesions of WT are so called nephrogenic rests and are defined as "a focus of abnormally persistent nephrogenic cells, meaning cells that can be induced to form a Wilms' tumor".<sup>3</sup>

Histologically, WT present with three distinct cell types: epithelial, stromal, and blastemal. All three elements are not required for diagnosis, but when all are present, the term "triphasic" is used. Heterologous components, including collagen, smooth muscle, skeletal muscle, cartilage, and bone may also

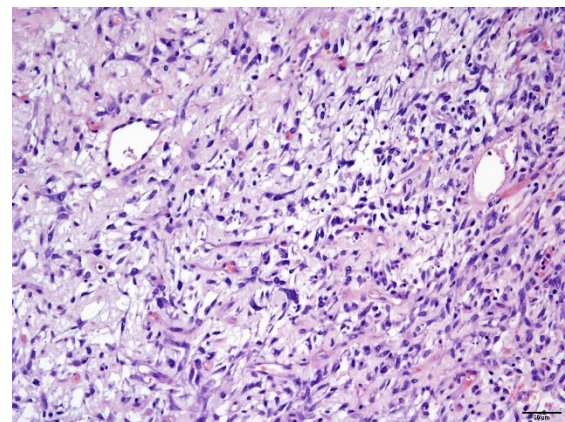


**Figure 3-4. Kidney, rat. The stromal population is composed of fusiform cells arranged in bundles and are supported by a loose fibrovascular stroma. (HE, 400X) (Photo courtesy of Laboratory of Comparative Pathology; Hospital for Special Surgery, Memorial Sloan Kettering Cancer Center, The Rockefeller University, Weill Cornell Medicine. <https://www.mskcc.org/research-areas/programs-centers/comparative-medicine-pathology>)**

be present. Zhuang et al. showed that the blastemal, epithelial, stromal, and other heterologous components of WT all have identical genetic changes, suggesting all features of this tumor are neoplastic.<sup>21</sup>

In laboratory animals, nephroblastomas have been frequently reported in rats, but are infrequent in mice and non-human primates.<sup>4,6</sup> In rats, nephroblastomas occur both experimentally and spontaneously. Experimentally, they can be induced by chemical administration of N-ethyl-N-nitrosourea or N-methyl-N-nitrosourea, both alkylating agents.<sup>20</sup> Spontaneously, they have been reported in Sprague-Dawley and F344 rats, with only rare reports of metastases to the lymph nodes and lungs.<sup>5,18</sup> No metastases were identified in our case.

The diagnosis of triphasic WT was based on the presence of blastemal, epithelial, and stromal components. Primitive tubular structures, surrounded by a rim of blastemal cells were identified, however, there was no evidence of primitive glomeruloid structures. In addition, there was widespread differentiation of the stromal components into striated

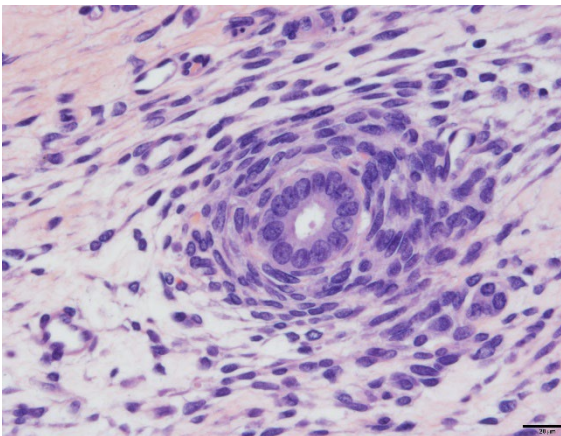


**Figure 3-5. Kidney, rat. The epithelial component is characterized by cuboidal to columnar cells which form tubules rimmed by a few layers of blastemal cells. (HE, 400X) (Photo courtesy of Laboratory of Comparative Pathology; Hospital for Special Surgery, Memorial Sloan Kettering Cancer Center, The Rockefeller University, Weill Cornell Medicine. <https://www.mskcc.org/research-areas/programs-centers/comparative-medicine-pathology>)**

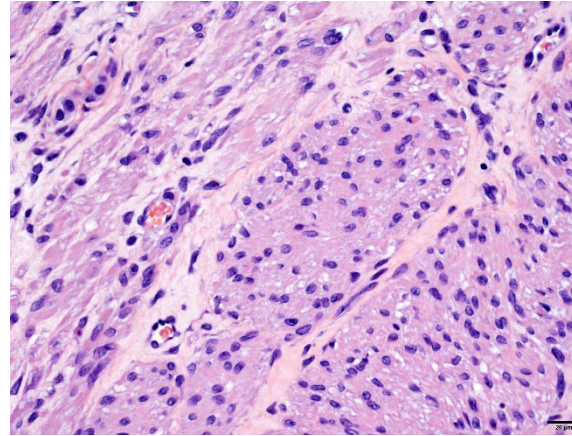


**Figure 3-6 Kidney, rat. The stromal population has large areas with heterologous smooth muscle differentiation. (HE, 400X) (Photo courtesy of Laboratory of Comparative Pathology; Hospital for Special Surgery, Memorial Sloan Kettering Cancer Center, The Rockefeller University, Weill Cornell Medicine. <https://www.mskcc.org/research-areas/programs-centers/comparative-medicine-pathology>)**

and smooth muscle, and collagen. The diagnosis of WT was aided by immunoreactivity of both blastemal and stromal populations with WT1, vimentin and immuno-negativity for cytokeratin WSS. The epithelial component was positive for cytokeratin, equivocally immunoreactive for WT1 and negative for vimentin. However, from our search, the veterinary literature is inconclusive regarding immunohistochemical profiles of these tumors, especially regarding the epithelial component. This may in part be due to the challenge in differentiating the epithelial population from the blastemal population, the choice of antibody, or the up/downregulation of certain proteins at different cellular developmental stages. In our case, the identification of epithelial components was simplified by the presence of discrete tubular structures, which were immunoreactive with cytokeratin WSS.

The main differential diagnosis for a WT is a renal mesenchymal tumor (RMT). RMTs arise from multipotential spindle-shaped mesenchymal cells, and, like WTs, can also give rise to heterologous components, such as smooth or skeletal muscle, fibrous tissue, cartilage and/or bone.<sup>17</sup> Further misleading

pathologists, profiles of hyperplastic tubules are frequently found in RMTs, but these are considered preexisting entrapped renal tubules, rather than newly formed. The pathognomonic feature of WT is the population of blastemal cells, which are immediately apparent in our case.

Finally, the significance of multiple, individual, partially developed, and variably sclerotic glomeruli, as well as variably sized tubules within the stromal population at the margins of the tumor is not determined. We suspect these may represent normal renal structures that were entrapped and separated from the renal parenchyma at the early onset of neoplasia. However, we cannot exclude that they may have arisen *de novo*.

#### **Contributing Institution:**

Laboratory of Comparative Pathology; Hospital for Special Surgery, Memorial Sloan Kettering Cancer Center, The Rockefeller University, Weill Cornell Medicine.  
<https://www.mskcc.org/research-areas/programs-centers/comparative-medicine-pathology>

#### **JPC Diagnosis:**

Kidney: Nephroblastoma.

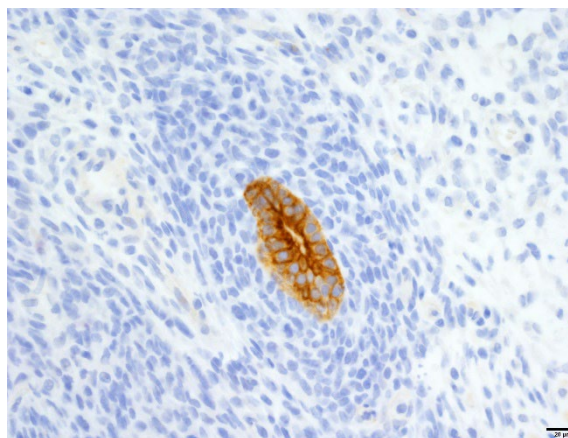


**Figure 3-7.** *Kidney rat. The tubular structures formed by the epithelial population have strong cytoplasmic immunoreactivity, while the surrounding blastemal cells are negative. Cytokeratin WSS IHC.*

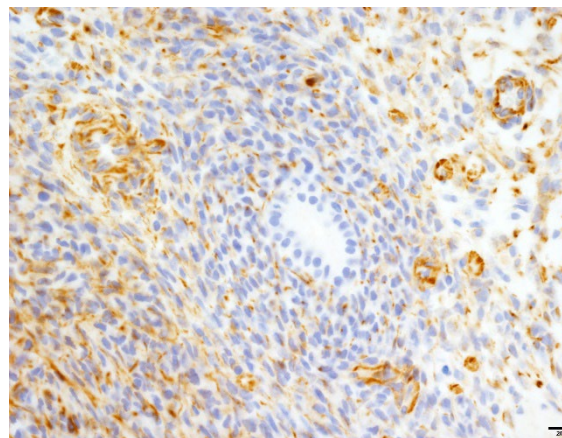


**Figure 3-8.** *Kidney, rat. The blastemal and stromal populations have moderate cytoplasmic immunoreactivity, while the tubular structures of the epithelial population are negative. Vimentin IHC.*

#### **JPC Comment:**

Nephroblastomas are the most common renal neoplasms in pigs, chickens, and fish.<sup>13</sup> In pigs, they generally exhibit a benign behavior.<sup>13</sup> Nephroblastomas also occur in a variety of other veterinary species, including dogs, cats, bovine fetuses, Japanese eels, guanacos, cottontail rabbits, and budgerigars.<sup>1,8,10,16</sup> In recent literature, a primary nephroblastoma was reported in the nasopharynx of a 3-month-old Boer goat, and unilateral stromal-type nephroblastomas were reported in the kidneys of two hedgehogs.<sup>2,19</sup>

In dogs, nephroblastomas are the third most common renal neoplasm, accounting for approximately 5% of renal neoplasia.<sup>13</sup> Up to 50% of canine nephroblastomas metastasize, and potential sites include the contralateral kidney, lung, liver, mesenteric lymph nodes, and spinal cord.<sup>7</sup> A recent report also described the first documented case of gingival metastasis in an 8 year old miniature Pinscher.<sup>7</sup> Primary spinal nephroblastomas also occur in young dogs, arising from nephrogenic rests between the dura and spinal cord, typically in the thoracolumbar region.<sup>12</sup> A recent report in a 1-year-old male American pitbull terrier documented multifocal spinal nephroblastomas arising in the thoracolumbar region, cervical intumescence, sacral

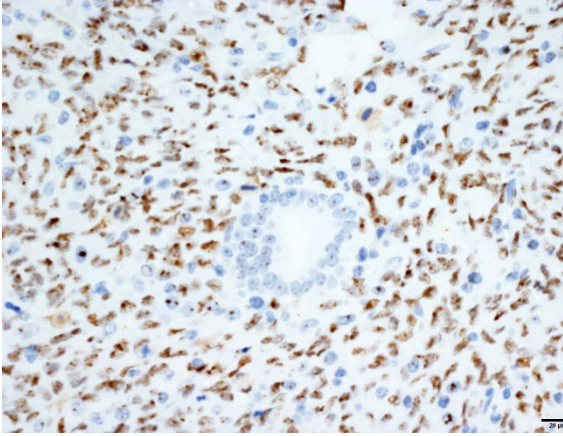


**Figure 3-9. Kidney, rat. The blastemal population has moderate, nuclear immunoreactivity, while the nuclear immunoreactivity of tubular structures is equivocal and appears to correspond to reactivity of nucleoli. WT1 IHC.**

segment, and cauda equina.<sup>11</sup> The authors believed that neoplastic seeding of the CNS resulted in the multifocal distribution, because vascular invasion was not observed but neoplastic cells expanded Virchow-Robbins spaces (which are continuous with the subarachnoid space).<sup>11</sup>

Differential diagnoses discussed by the contributor included renal cell carcinoma, renal mesenchymal tumor, amphophilic vacuolar tumor, renal sarcoma, and liposarcoma; diagnostic criteria for the tumors can be reviewed on the Global Open Registry Nomenclature Information System at goRENI.org.

#### References:

1. Agnew D. Camelidae. In: Terio KA, McAloose D, St. Leger J, eds. *Pathology of Wildlife and Zoo Animals*. San Diego, CA: Elsevier. 2018; 193.
2. Athey JM, Rice LE, Harvey AB, Washburn KE, Rodrigues-Hoffman A. Nasopharyngeal nephroblastoma in a 3-month-old Boer goat. *J Vet Diagn Invest*. 2021; 33(1):108-111.
3. Beckwith J, Bruce NB, Bonadio K. Nephrogenic rests, nephroblastomatosis, and the pathogenesis of Wilms' tumor. *Pediatr Pathol*. 1990; 10:1-36.

4. Castiglioni V, De Maglie M, Queliti R. Immunohistochemical characterization of a renal nephroblastoma in a trp53-mutant and prolyl isomerase 1-deficient mouse. *J Toxicol Pathol*. 2013; 26:423-427.
5. Chandra M, Carlton WW. Incidence, histopathologic and electron microscopic features of spontaneous nephroblastomas in rats. *Toxicol Lett*. 1992; 62: 179-190.
6. Chandra M, Riley MGI, Johnson DE. Spontaneous renal neoplasms in rats. *J Appl Toxicol*. 1993; 13:109-116.
7. Chen B, Li W, Wang F. A blastema-predominant canine renal nephroblastoma with gingival metastasis: case report and literature review. *J Vet Diagn Invest*. 2018; 30(3): 430-437.
8. Delaney MA, Treuting PM, Rothenburger JL. Lagomorpha. In: Terio KA, McAloose D, St. Leger J, eds. *Pathology of Wildlife and Zoo Animals*. San Diego, CA: Elsevier. 2018; 486.
9. Dumba M, Jawad N, McHugh K. Neuroblastoma and nephroblastoma: an overview and comparison. *Cancer Imaging*. 2014; 14:O15.
10. Frasca Jr S, Wolf JC, Kinsel MJ, Camus AC, Lombardini ED. Osteichthyes. In: Terio KA, McAloose D, St. Leger J, eds. *Pathology of Wildlife and Zoo Animals*. San Diego, CA: Elsevier. 2018; 961.
11. Henker LC, Bianchi RM, Vargas TP, de Oliveira EC, Driemer D, Pavarini SP. Multifocal Spinal Cord Nephroblastoma in a Dog. *J Comp Path*. 2018; 158: 12-16.
12. Higgins RJ, Bollen AW, Dickinson PJ, Siso-Llonch S. *Tumors of the Nervous System*. In: Meuten DJ, ed. *Tumors in Domestic Animals*. 5th ed. Ames, Iowa: Iowa State Press; 2017
13. Meuten DJ, Meuten TLK. Tumors of the urinary system. In: Meuten DJ, ed. *Tumors in Domestic Animals*. 5th ed. Ames, Iowa: Iowa State Press; 2017:646-649.

14. Pritchard-Jones K. Malignant origin of the stromal component of Wilms' tumor. *J Natl Cancer Inst.* 1997; 89:1089–1091.
15. Pritchard-Jones K, Vujanic G. Multiple pathways to Wilms tumor: how much is genetic?. *Pediatr Blood Cancer.* 2006; 47:232-234.
16. Reaville DR, Dorrenstein G. Psittacines, Coliiformes, Musophagiformes, Cuculiformes. In: Terio KA, McAloose D, St. Leger J, eds. *Pathology of Wildlife and Zoo Animals.* San Diego, CA: Elsevier. 2018; 784.
17. Seely JC. Renal mesenchymal tumor vs nephroblastoma: revisited. *J Toxicol Pathol.* 2004; 17: 131-136.
18. Tanaka, N, Takeshi I, Jyoji Y. Spontaneous nephroblastoma with striated muscle differentiation in an F344 rat. *J Toxicol Pathol.* 2017; 30:231-234.
19. Ueda K, Imada T, Ueda A, Imada M, Ozaki K. Stromal-type Nephroblastoma with or without Anaplasia in Two Hedgehogs. *J Comp Path.* 2019; 172: 48-52.
20. Yoshizawa K, Kinoshita Y, Emoto Y. N-Methyl-N-nitrosourea-induced Renal Tumors in Rats: Immunohistochemical Comparison to Human Wilms Tumors. *J Toxicol Pathol.* 2014; 26:141-148.
21. Zhuang Z, Merino MJ, Vortmeyer AO. Identical genetic changes in different histologic components of Wilms' tumors. *J Natl Cancer Inst.* 1997; 89:1148-52.

#### **CASE IV:**

##### **Signalment:**

Adult, female, Sprague Dawley rat, *Rattus norvegicus*

##### **History:**

The animal was in the control group on a 5-week general toxicology study. The animal was dosed with vehicle via oral gavage and had no notable clinical signs.

##### **Gross Pathology:**

There were no significant gross lesions.

##### **Laboratory Results:**

There were no abnormalities on urinalysis, serum chemistry, or hematology.

##### **Microscopic Description:**

In a section of kidney, at the junction of the medulla and cortex are multifocal areas of proliferative stellate to polygonal blastemal cells separating and infiltrating between normal fully developed tubules supported by a small amount of fine fibrovascular stroma. The blastemal cells have a small amount of pale basophilic cytoplasm, have indistinct cell borders, and are arranged in streams, nests, rosettes, and irregular tubules. The tubules are lined by a single layer of epithelial cells or are piled haphazardly. The cells have ovoid nuclei with finely stippled chromatin and 1-3 nucleoli. There are 1-2 mitoses per high power (400x) field. Small numbers of lymphocytes infiltrate these areas. Adjacent areas of the medulla and cortex appear unaffected.

##### **Contributor's Morphologic Diagnoses:**

Kidney: Multifocal nephroblastematosi

##### **Contributor's Comment:**

Nephroblastematosi is a spontaneous/inci-

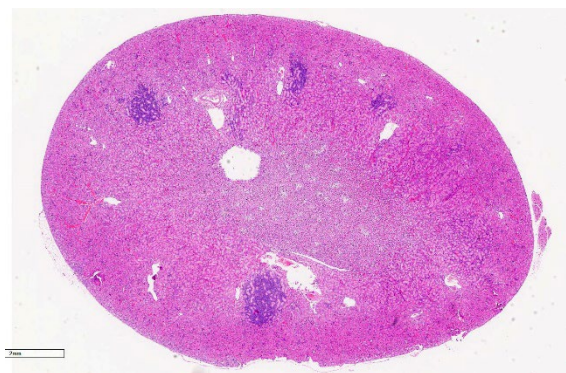


**Figure 4-1. Kidney, rat. One section of kidney is submitted for examination. There are multiple hypercellular foci within the cortex. (HE, 5X) (Photo courtesy of: Charles River Laboratories, Mattawan, MI)**

idental lesion that can be encountered in rats

in toxicologic studies.<sup>2</sup> This condition is also known as nephroblastomatosis, blastemal rest, nephrogenic rest, or intralobar nephroblastomatosis and has been reported in rats, dogs, and human children.<sup>2,5,6,7</sup> Nephroblastomatosis can be encountered in any age of rat and may have the potential to develop into nephroblastomas as the lesions enlarge; thus, they are regarded as preneoplastic lesions.<sup>1,2,6,7</sup> These lesions are not grossly apparent, and by the time the lesions are large enough to be observed grossly, they are more consistent with a diagnosis of nephroblastoma.<sup>7</sup>

As described, the lesions are composed of microscopic masses at the corticomedullary junction composed of dense blastemal cells with scant basophilic cytoplasm and basophilic nuclei (Figure 1).<sup>2</sup> There may be rare renal organoid differentiation into rosettes, glomeruloid structures and tubules (Figure 2).<sup>2</sup> Adjacent pars recta tubules may have mitotic figures, which is an autocrine response to the blastema.<sup>1</sup> These lesions usually do not cause severe disruption of the surrounding kidney architecture, though may be associated with dilated tubules.<sup>7</sup>

Nephroblastoma is the main differential for this lesion, though the delineation between these findings appears arbitrary and based on size and degree of organoid differentiation such as more tubules and glomerular structures.<sup>2,7</sup> Nephroblastomatosis also usually presents with a multifocal nature, as in this case.<sup>2</sup>

In humans, nephrogenic rests are differentiated into incipient, dormant, involuting, hyperplastic, or neoplastic rests.<sup>1,5</sup> Incipient rests have microscopic evidence of proliferation or maturation and are seen in infants.<sup>5</sup> Dormant rests are present in older people and may remain unchanged for years.<sup>1,5</sup> Involuting, also known as sclerosing or obsolescent,

rests are composed of a well-formed tubule lined by a single layer of low-cuboidal epithelium surrounded by dense collagen, and may eventually disappear.<sup>1,5</sup> Hyperplastic rests exhibit proliferation in diffuse or focal areas and may progress to grossly apparent masses.<sup>1</sup> Neoplastic rests are those in which neoplastic transformation occurs within single cells of the rest which go on to produce Wilms tumor.<sup>1</sup> These rests can also be separated into perilobar or intralobar nephrogenic rests.<sup>1</sup> Perilobar nephrogenic rests occur at the periphery of the lobe, whereas intralobar rests occur anywhere within the lobe.<sup>1</sup> In humans, intralobar nephrogenic rests have been associated with loss or mutation of the WT1 gene.<sup>1</sup>

Some authors refer to nephroblastomatosis in rats, which have a unilobar kidney, as intralobar nephroblastomatosis as the blastemal cells occur within the lobule at the corticomedullary junction.<sup>7</sup> While some authors consider the terms nephroblastomatosis and nephroblastomatosis to be synonymous, others consider the terminology nephroblastomatosis to represent multiple grossly apparent nephroblastomas.<sup>2,7</sup> Nephroblastomatosis is the preferred terminology by the International Harmonization of Nomenclature and Diagnostic Criteria for Lesions in Rats and Mice (INHAND) Project and Standardization for Exchange of Nonclinical Data (SEND).<sup>2</sup>

#### **Contributing Institution:**

Charles River Laboratories, Mattawan, MI

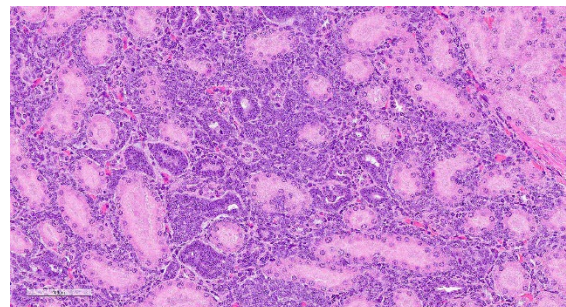


**Figure 4-2.** Kidney, rat. Tubules are surrounded and separated by blastemal cells. (HE, 200X) (Photo courtesy of: Charles River Laboratories, Mattawan, MI)

### JPC Diagnosis:

Kidney: Nephroblastematosi s, multifocal.

### JPC Comment:

The contributor provides a thorough description of an uncommonly documented lesion in veterinary species, and this case of nephroblastematosi s provides a glimpse of pre-neoplastic changes which may have proceeded the nephroblastoma from Case 3 of this conference.

Nephroblastematosi s was first described in a 1961 report of a premature human infant at 32 weeks gestation.<sup>4</sup> The cortical surfaces were enlarged and slightly lobulated, and they kidneys were histologically consistent with 14-16-week gestational age, with blastemal cells surrounding areas of stroma, tubules, and glomeruli.<sup>4</sup> In that case, both kidneys were diffusely affected, but it is now known that nephroblastematosi s more commonly occurs focally or multifocally.<sup>4</sup> During normal embryogenesis, migration of the ureteric bud into the metanephric blastema induces development of glomeruli, nephrons, and stroma.<sup>4</sup> Defects earlier in nephrogenesis result in the failure of differentiation in intralobular nephrogenic rests, while later defects result in persistent perilobular rests.<sup>4</sup> Nephroblastematosi s occurs when nephrogenic rests persist beyond 34-36 weeks gestation in humans.<sup>4</sup> Nephrogenic rests are found in approximately 1% of all human pediatric autopsies, with perilobar the most common location.<sup>4</sup> All nephrogenic rests

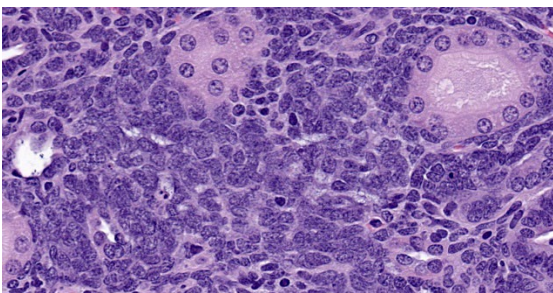


**Figure 4-3. Kidney, rat. High magnification of blastemal cells. (HE, 400X)**

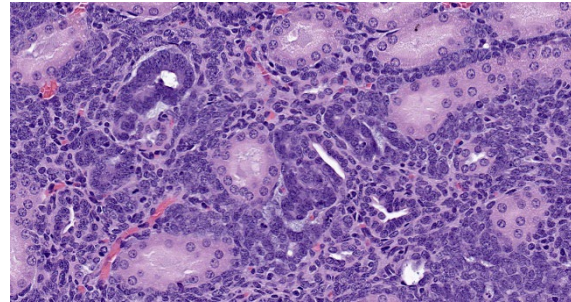


**Figure 4-4. Kidney, rat. Blastemal cells multifocal differentiate into tubules. (HE, 400X)**

have the potential to become neoplastic, either as adenomas (i.e. metanephric adenoma or adenofibroma) or nephroblastomas.<sup>4</sup> In humans, however, regression is much more common, and only approximately 1% progress to neoplasia.<sup>4</sup>

As the contributor alludes to, differentiating nephroblastematosi s and nephroblastoma is challenging. In humans, nephrogenic rests generally have irregular margins, lack encapsulation, may have foci of sclerosis between rests, whereas nephroblastomas are generally round with pseudoencapsulation and may lack sclerosis.<sup>4</sup> Pre-existing non-neoplastic blastema may be found along the periphery of nephroblastomas.<sup>4</sup> Conference participants remarked about the presence of irregular tubules which could lead a pathologist to diagnose nephroblastoma, but elected to follow criteria from human literature described above.

Reports of nephroblastematosi s are very rare in veterinary species, and the contributor covers this condition in rats well. Additionally, nephroblastematosi s has also been described as an incidental finding in a single cynomolgus macaque.<sup>3</sup>

### References:

1. Beckwith JB. Nephrogenic rests and the pathogenesis of Wilms tumor: Developmental and clinical consideration. *Am J Med Genet.* 1998;79:268-273.
2. Frazier KS, Seely, JC, Hard GC, et al. Proliferative and nonproliferative lesions

of the rat and mouse urinary system. *Tox Pathol.* 2012;40:14S-86S.

3. Goens SD, Moore CM, Brasky KM, et al. Nephroblastomatosis and nephroblastoma in nonhuman primates. *J Med Primatol.* 2005; 34: 165-170.
4. Hennigar RA, O'Shea PA, Grattan-Smith JD. Clinicopathologic features of nephrogenic rests and nephroblastomatosis. *Adv Anat Pathol.* 2001; 8(5):276-89.
5. Jackson CB and Kirkpatrick JB. Nephrogenic rest in a Crl:CD (SD)IGS BR rat. *Vet Pathol.* 2002;39:588-589.
6. Kelaiselvan P, Mathur KY, Pande VV, et al. Intralobar nephroblastematosi s in a nine-week-old Wistar rat. *Tox Pathol.* 2009;37:819-825.
7. Mesfin GM. Intralobar nephroblastematosi s: Precursor lesions of nephroblastoma in the Sprague-Dawley Rat. *Vet Pathol.* 1999;36:379-390.